SAND2022-12087C

Sandia National Laboratories

Aerosol deposition of thermographic phosphors for non-contact, simultaneous temperature and strain measurements

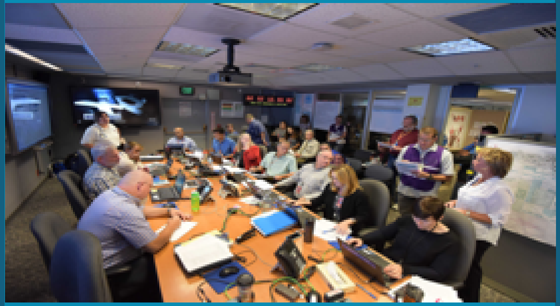

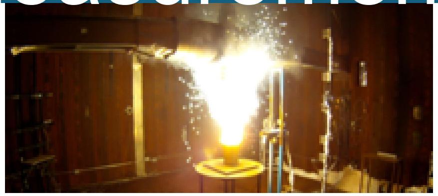

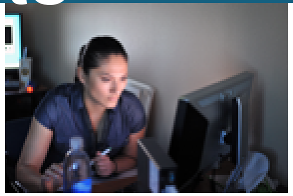

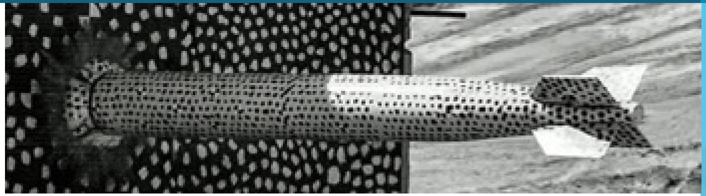

September 14, 2022

Presented by Shannon Murray

This work was supported by the Laboratory Directed Research and Development program at Sandia National Laboratories, a multimission laboratory managed and operated by National Technology and Engineering Solutions of Sandia LLC, a wholly owned subsidiary of Honeywell International Inc. for the U.S. Department of Energy's National Nuclear Security Administration under contract DE-NA0003525.

Sandia National Laboratories is a multimission laboratory managed and operated by National Technology & Engineering Solutions of Sandia, LLC, a wholly owned subsidiary of Honeywell International Inc., for the U.S. Department of Energy's National Nuclear Security Administration under contract DE-NA0003525.

Sandia National Laboratories – Albuquerque, NM

Thermal Spray Research Laboratory (TSRL)

Aerosol Deposition (AD)

Thermographic phosphors for non-contact, simultaneous temperature and strain measurements

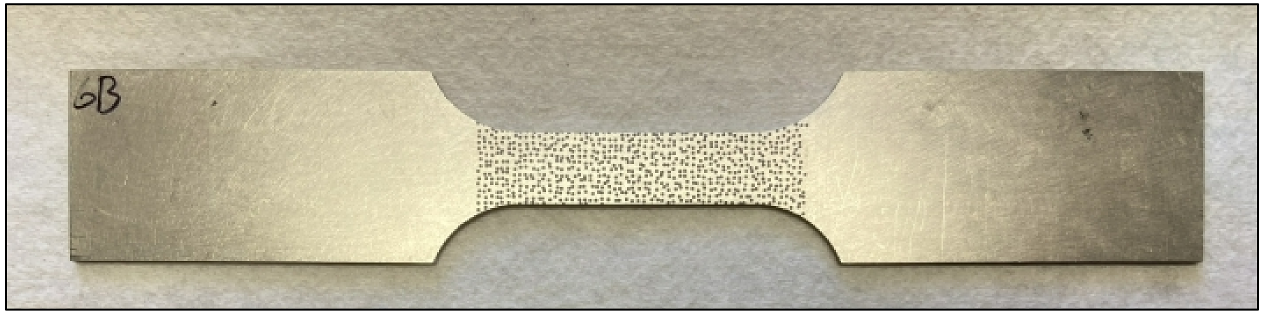

Outline

Background

1. Thermal Spray Research Laboratory
2. Aerosol Deposition
3. Thermographic phosphors

Previous Results

4. Deposition details
5. Temperature + strain measurements

Current Efforts

6. In-situ tensile test

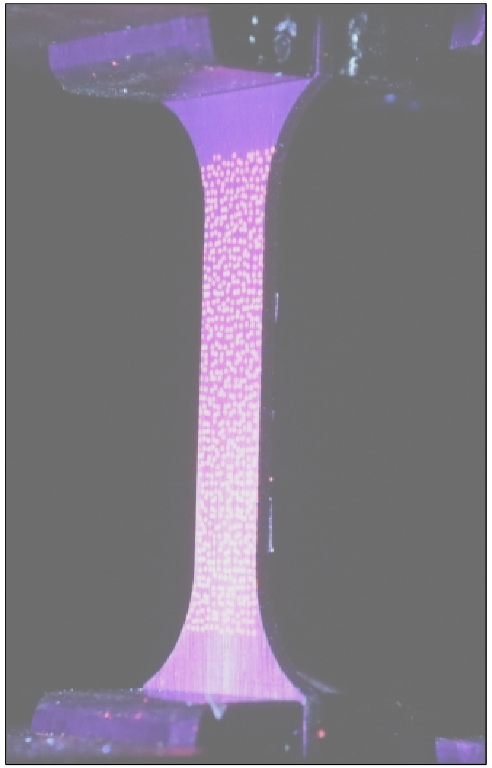

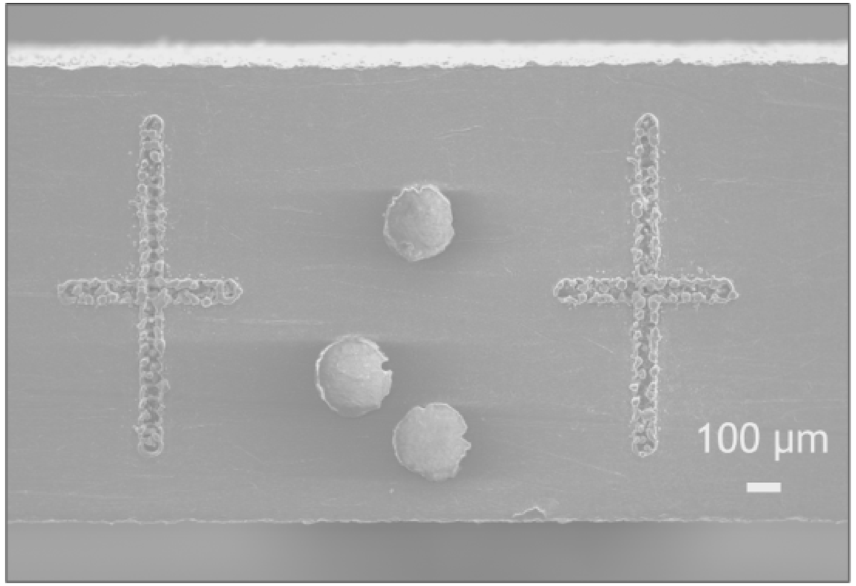

Thermal Spray Research Laboratory (TSRL)

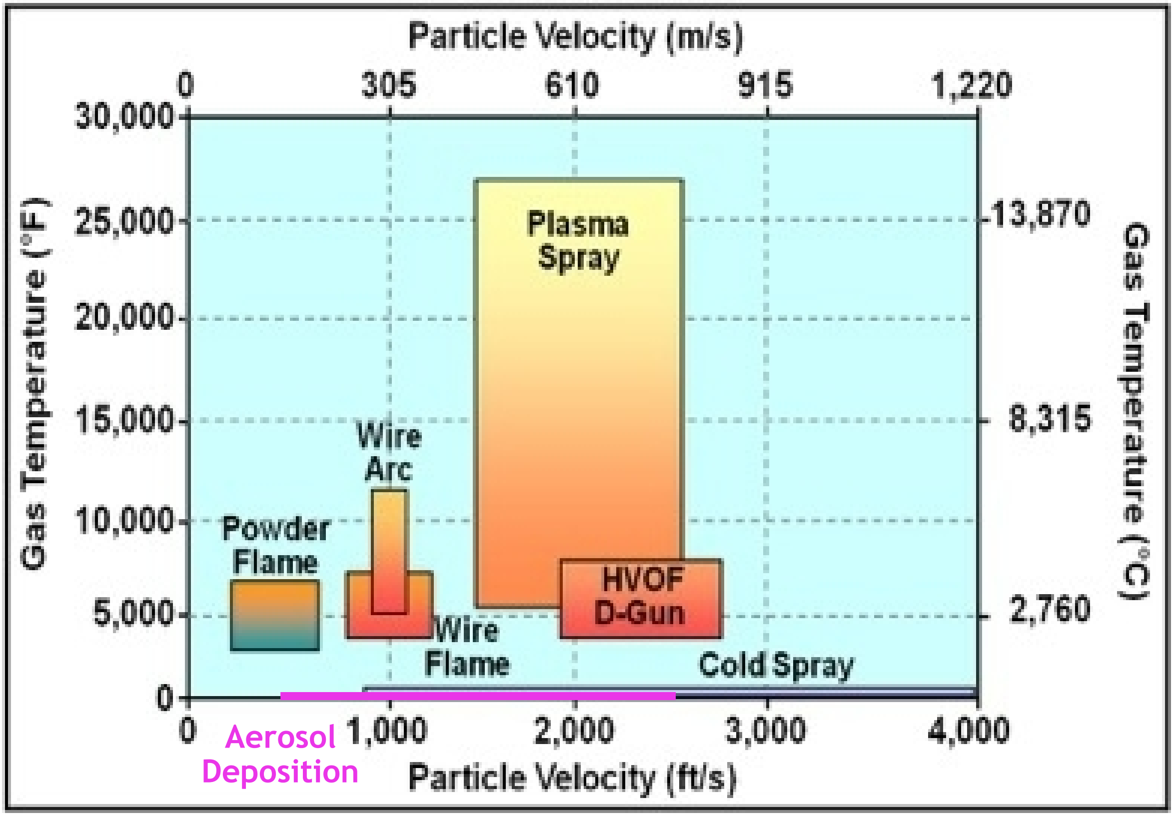

*Adapted from plots by R.C. McCune, Ford Motor Co. & A. Papyrin, Ktech Corp.
R. Dykhuizen, et al., *JTST*, 2, 1998

Spray techniques available at TSRL

Twin Wire Arc Spray

Air Plasma Spray

Controlled Atmosphere Plasma Spray

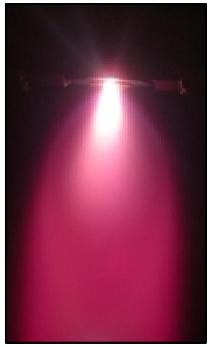

Powder Flame Spray

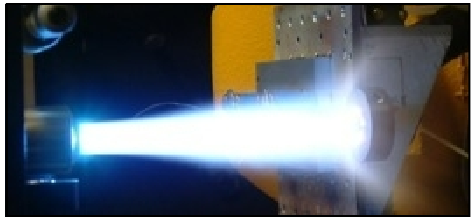

Cold Spray (CS)

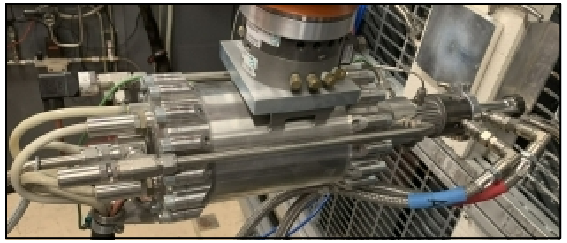

Aerosol Deposition (AD)

AD is a kinetic spray process similar to CS

For both CS and AD:

- Feedstock powder is not melted
- Coating is built through impact consolidation
- Converging/diverging nozzle is used

Cold Spray

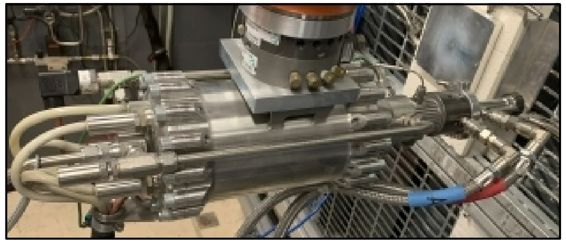

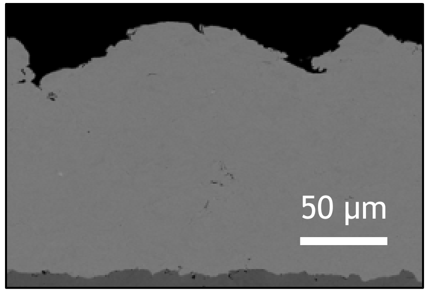

Courtesy of Mike Kracum

- Gas is heated (generally 600°C – 800°C)
- Larger particles (15 - 45 microns)
- Performed in air
- Coating thickness:
  - 20 microns - 10 mm
- Coating materials: metal, metal composites
- Substrate materials: metal

Aerosol Deposition

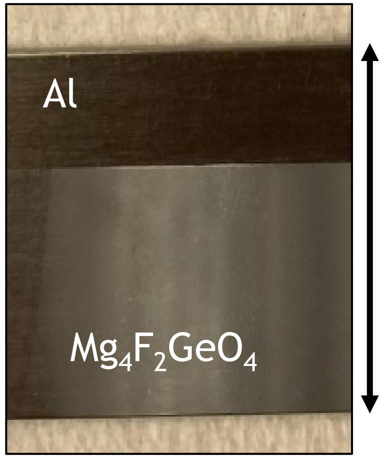

- Room temperature
- Smaller particles (600 nm – 1 micron)
- Performed under vacuum
- Coating thickness:
  - Metal: 10 microns – 2.5 mm thick
  - Ceramic: 1 - 150 microns thick
- Coating materials: metal, ceramic, cermet, polymer
- Substrate materials: metal, ceramic, polymer

AD can deposit pure ceramic coatings

AD has been used to produce functional ceramic coatings

Room Temperature Deposition of Ceramics

- Temperature-sensitive substrates can be coated with refractory materials
- Oxidation and phase transformations due to melting and resolidification are avoided

Scanning electron microscope (SEM) image of cross section

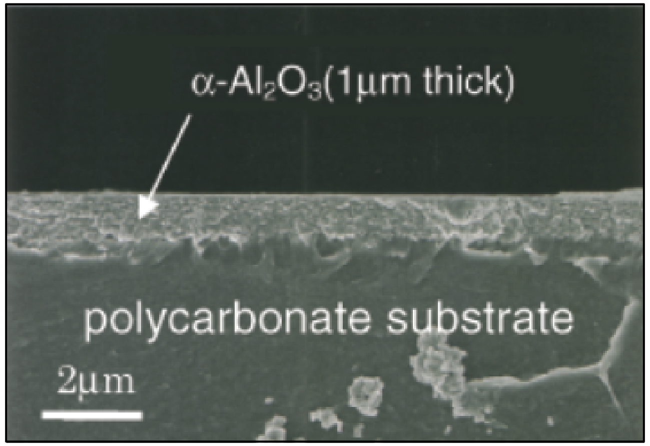

J. Akedo, *J. Am. Ceram. Soc.*, **89**, 6, 1834–1839, 2006

Functional Coatings: Humidity Sensor

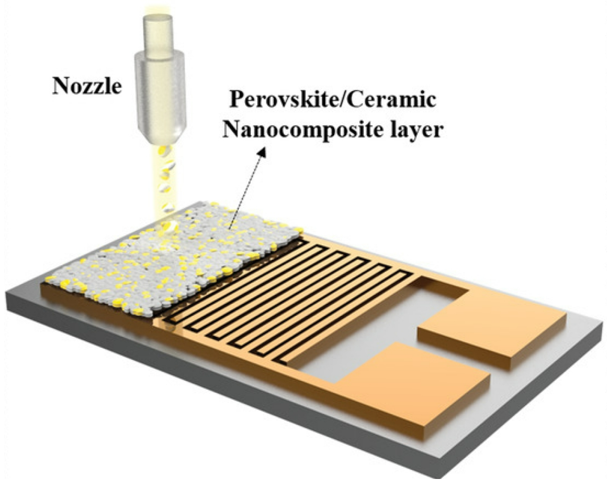

- Utilize porous microstructure for capacitive-type humidity sensor
- $CsPb_2Br_5/BaTiO_3$ (perovskite-based) nanocomposite
- Significant increase in humidity sensing compared with $CsPbBr_3/Al_2O_3$ and $CsPbBr_3/TiO_2$ sensors
- High sensitivity, superior linearity, fast response/recovery time, low hysteresis, excellent stability in a wide relative humidity range

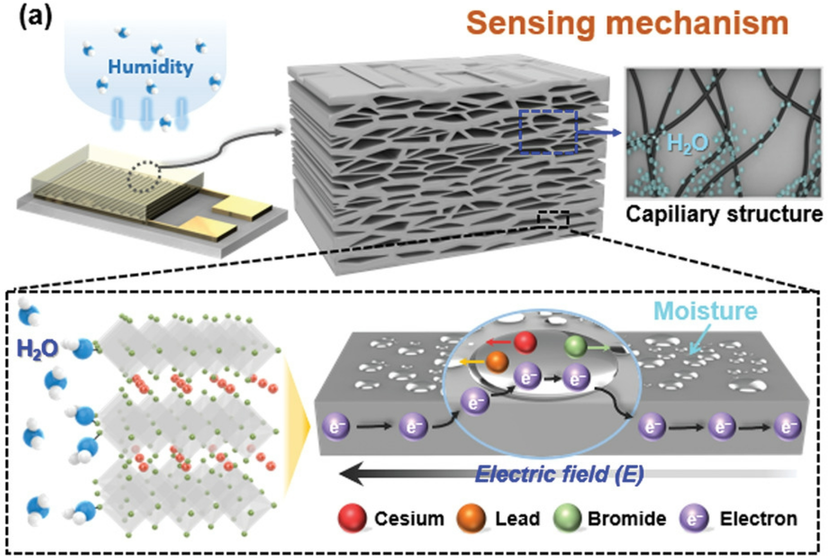

SEM image of $CsPb_2Br_5/BaTiO_3$ cross section (inset is surface image)

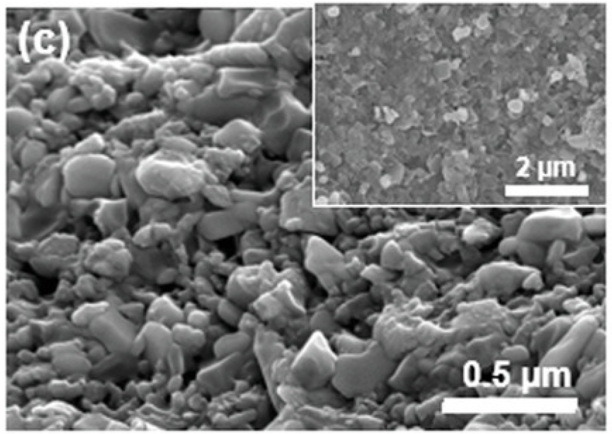

M. Cho, et al., *Adv. Funct. Mater.*, **30**, 1907449, 2020

AD is a versatile technique where coatings can be tailored to produce functional devices

AD at TSRL

A rotating brush generator provides constant powder feed rate and the ability to calculate the powder mass flow rate

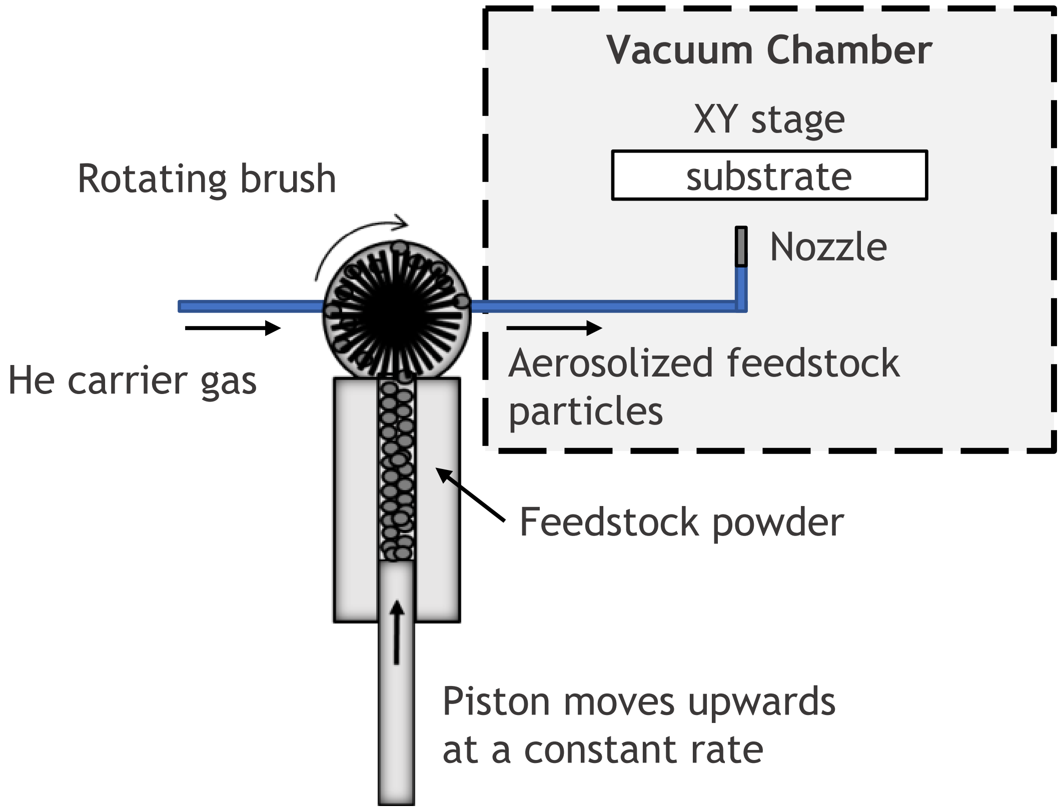

Rotating Brush Generator (RBG) 1000 ISD

Constant powder feed rate

5 – 700 mm/hr

Powder mass flow rate can be calculated

0.04 – 430 g/hr (for an assumed compacted density of 1 g/cm^3)

Spray Process Parameters

- Feed Rate: 20 mm/hr (~3000 mm^3/hr, 0.112 g/min)
- Carrier Gas: He
- Inlet Pressure: 15 psi
- Raster Rate: 900 mm/min
- Step Size: 1.2 mm
- Standoff Distance: 20 mm

Interchangeable nozzles allow for a wide range of particle velocities

Aerosolized, micron-sized particles are accelerated into a vacuum chamber and impact a substrate to form a coating.

Varying the diverging length of the nozzle modifies the particle velocity

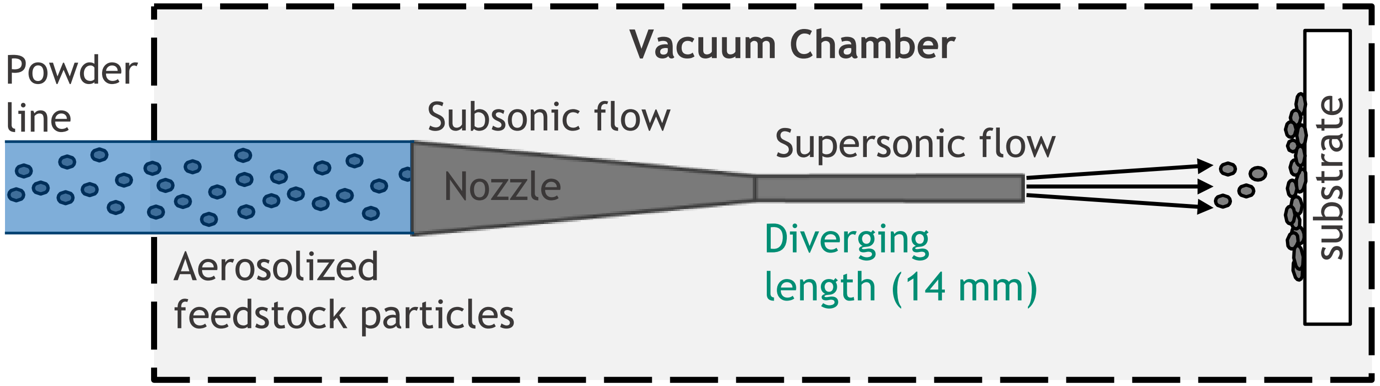

Increasing the diverging length increases the particle velocity.

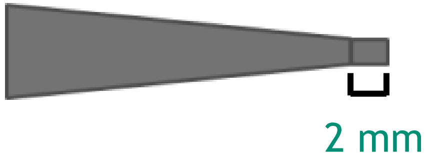

2.5 µm Al_2O_3, particle velocity = **304 m/s**

2.5 µm Al_2O_3, particle velocity = **825 m/s**

Highly tailorable process → capable of producing a wide variety of coatings

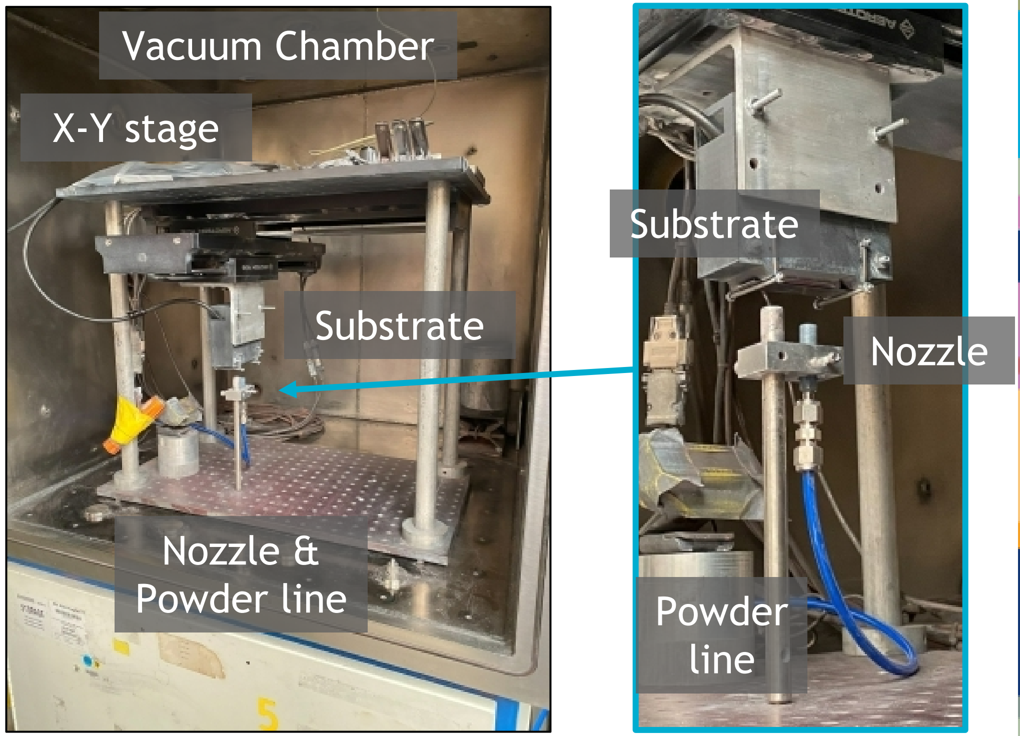

3D printed polymeric nozzles → rapidly produced

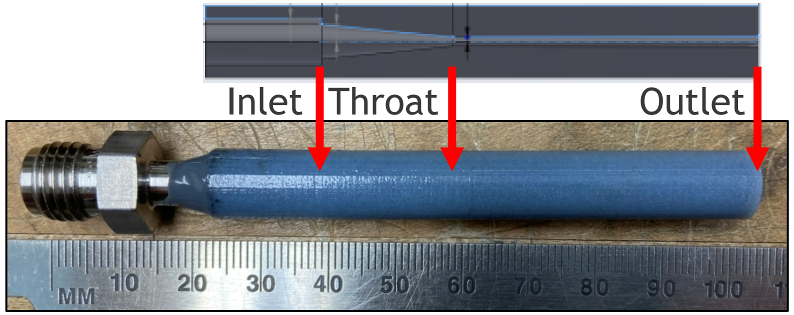

Development of thermometry using thermographic phosphors

Phosphor-coated Sample

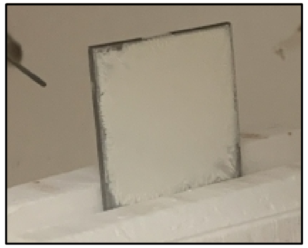

UV Excitation

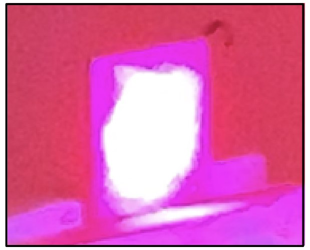

Visible Emission

UV light is used to excite activator atoms which remain in an elevated electronic state for a certain amount of time before relaxing back to the ground state by emitting visible photons

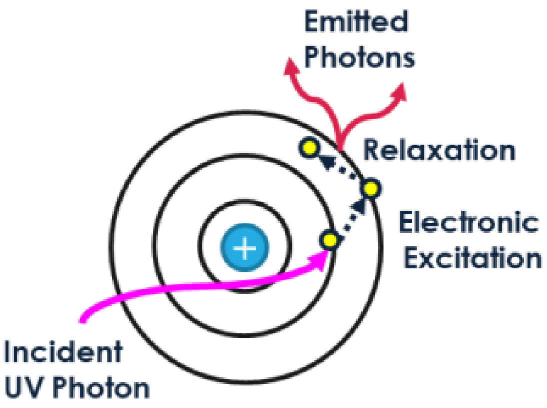

Transition or rare earth element-doped ceramics

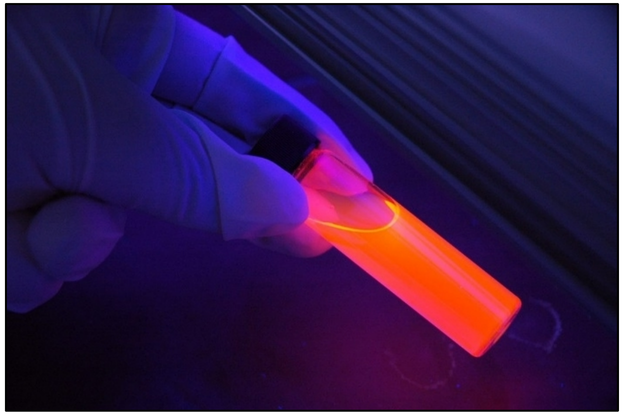

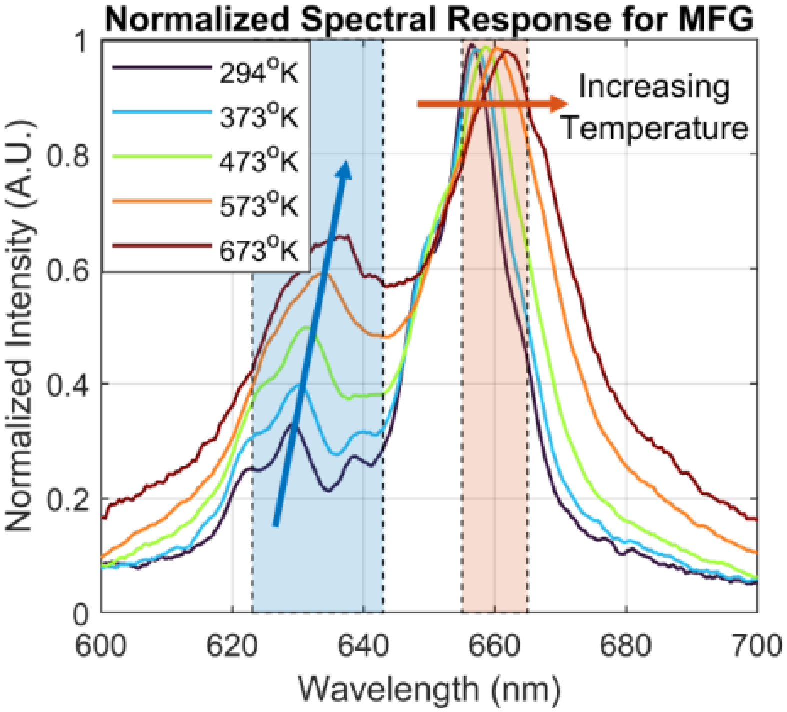

$Mg_4F_2GeO_4$:Mn (MFG)

Ratio of blue-to-red signal produces full-field temperature

$$\frac{I_b}{I_r} \propto T$$

The spectral emission is temperature dependent
→ Infer temperature from a single spectra (mean measurement over the area)

Use two cameras (each with a unique wavelength filter)
→ Infer temperature of the area via pixel-to-pixel correlation

Jones, E. M. C., *Strain* 2022

Thermographic Phosphor vs Conventional Temperature Measurement Devices

Thermographic phosphors

- Remote sensing
- Robust application
- Full-field sensing

Thermocouples (TC)

- Susceptible to loss of contact
- Intrusive
- Restricted to surface point measurement

Thermographic phosphors

- Can sense through optically thicken environments (ex. sooty fires)

Infrared (IR) camera

- Susceptible to background emission
- Must account for changing material emissivity
- Can suffer from image saturation
- Can suffer from biased measured temperature due to reflections from radiant heat

Aluminum Composite Coupons, Post-burn

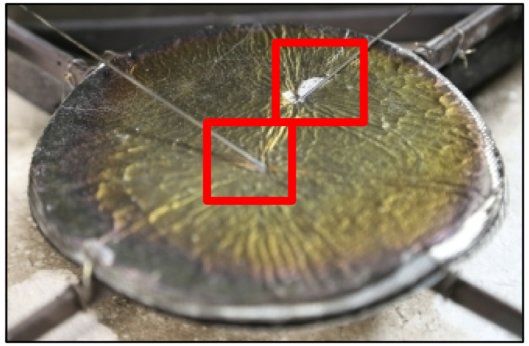

Intrusive puncture

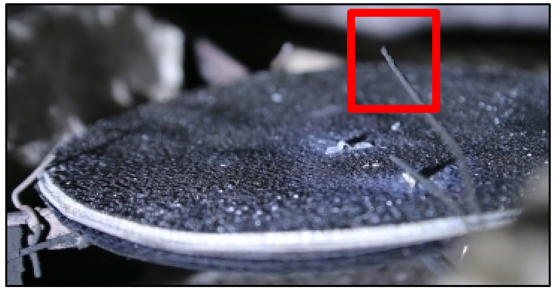

Loss of TC contact

Small Methane Pool Fire

IR Camera

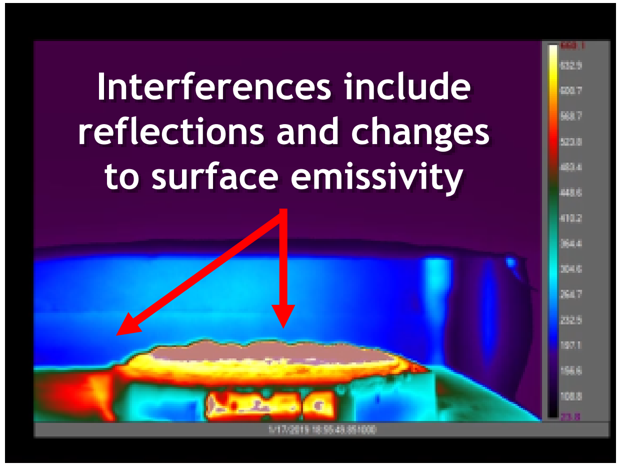

Thermographic phosphors expand the application space for temperature measurements

C. Winters

Outline

Background

1. Thermal Spray Research Laboratory
2. Aerosol Deposition
3. Thermographic phosphors

Previous Results

4. Deposition details
5. Temperature + strain measurements

Current Efforts

6. In-situ tensile test

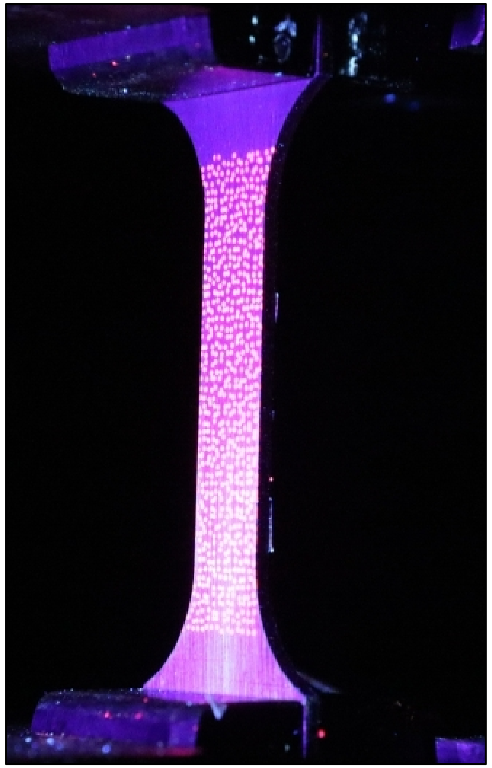

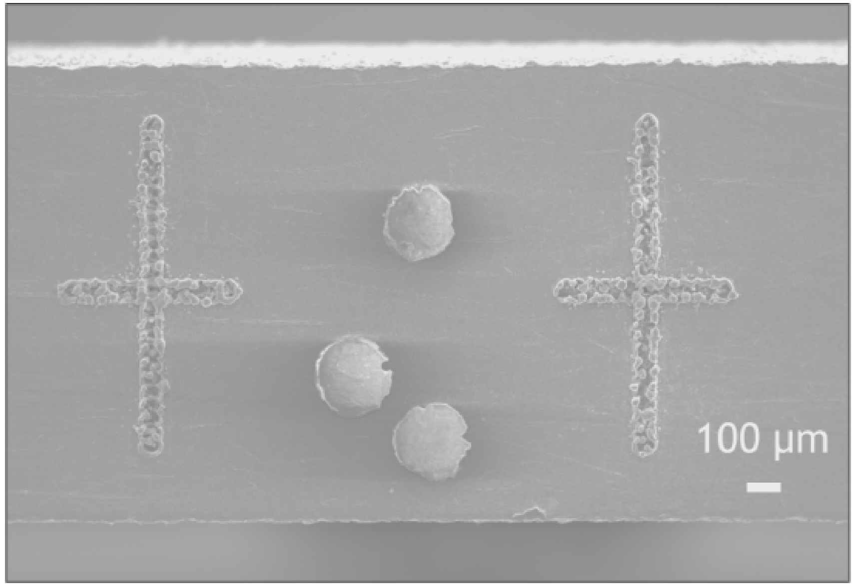

AD produces thin, robust, adherent coatings

Drawbacks of conventional techniques

(ex. ethanol "paint", phosphor + binder)

- Uneven distribution (difficult to control thickness)
- Poor adhesion
- Binder is flammable at high temperatures
- May require a thicker coating for sufficient signal to noise

Benefits of AD

- Thin, dense, and tailorable coatings
  → Faster thermal response time
- Faster data acquisition rates
  → Probe more dynamic events
- Robust coatings
  → Improved stability for thermal environments

Improved density, thermal conductivity, and purity of YAG:Dy (yttrium aluminum garnet) compared to conventional methods (paint, epoxy)

→ Higher thermal conductivity leads to improved temperature sensing

AD (500°C) Epoxy (400°C)

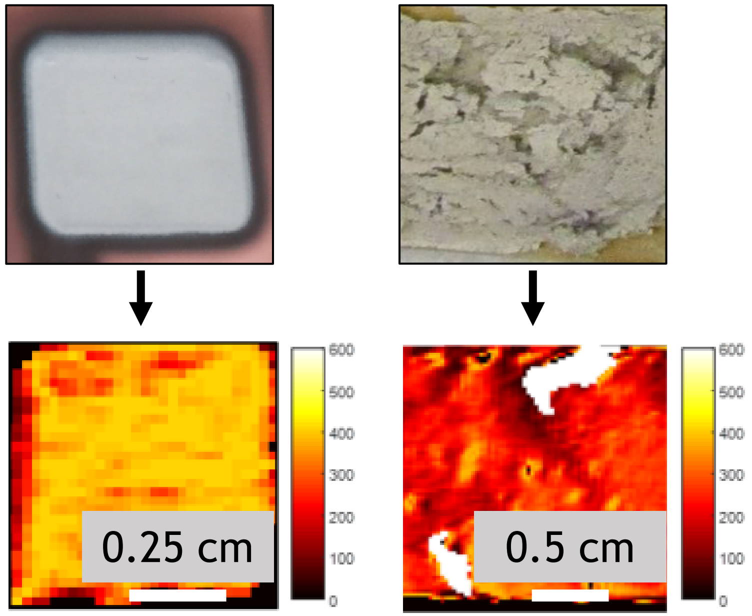

2-D temperature profiles

~250µm/pixel

AD surpasses conventional deposition methods producing robust coatings ideal for thermographic phosphor devices

Thermophosphor Experimental Setup

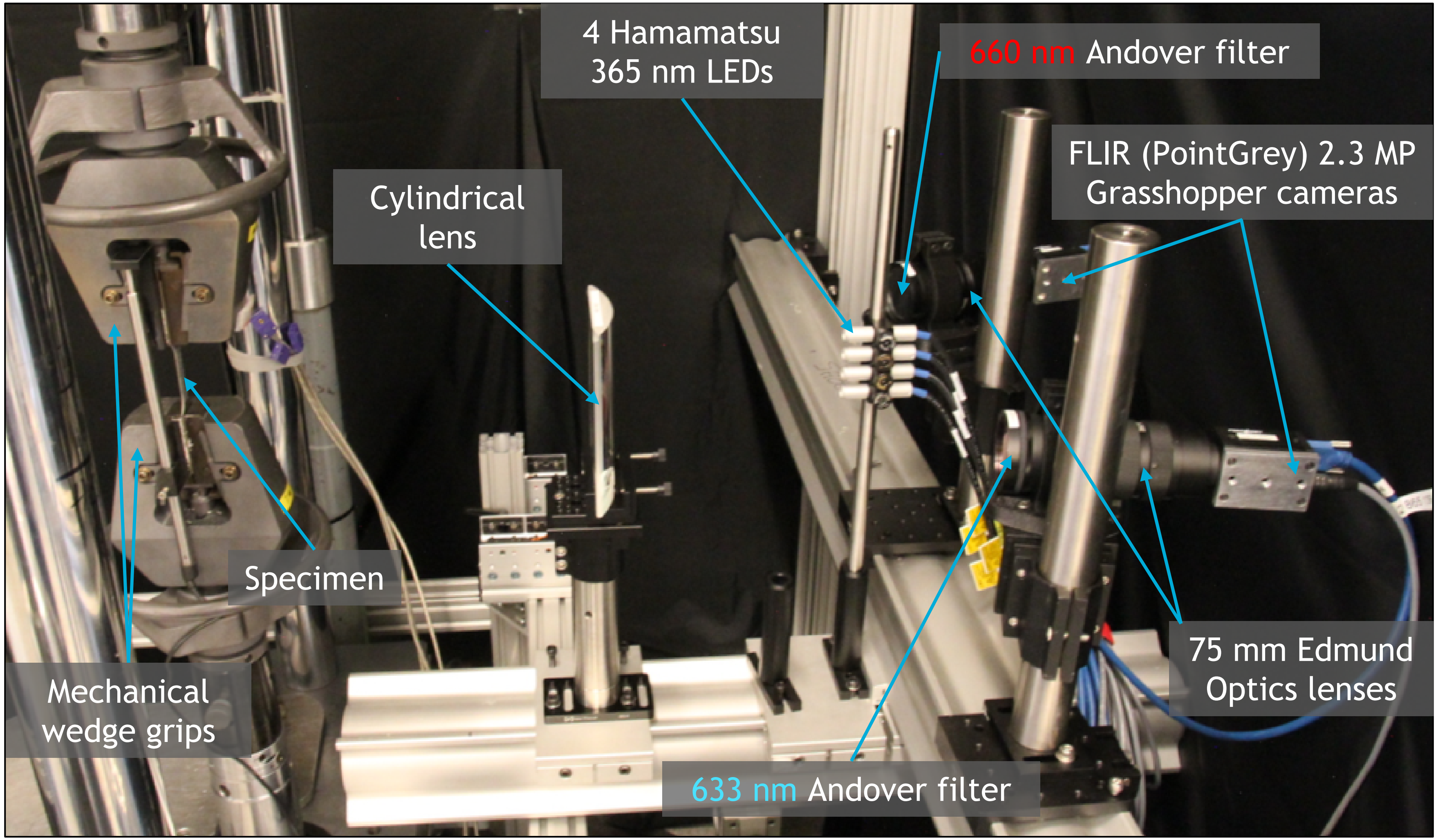

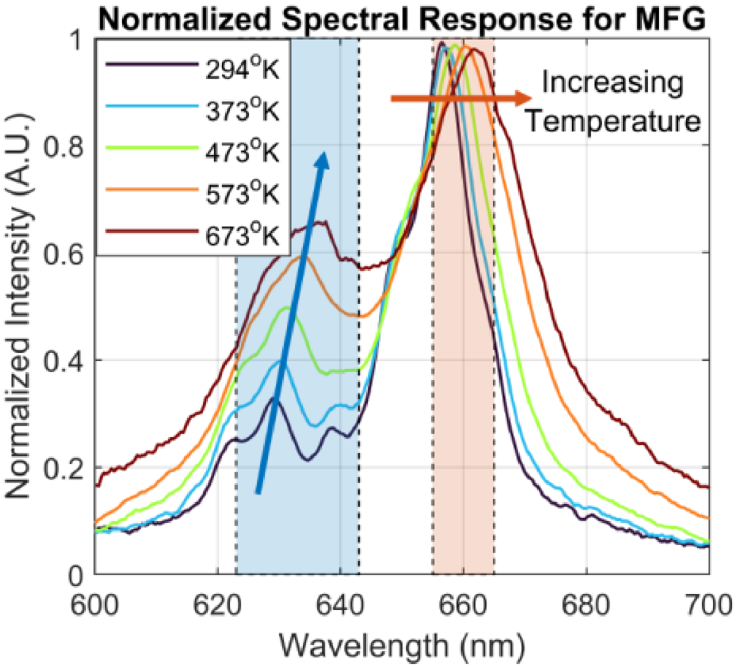

Ratio of blue-to-red signal produces full-field temperature

$$\frac{I_b}{I_r} \propto T$$

Use two cameras (each with a unique wavelength filter)
→ Infer temperature of the area via pixel-to-pixel correlation

E. Jones, C. Winters

Highly Sensitive and Uniform Temperature Measurements

Calibration Sample

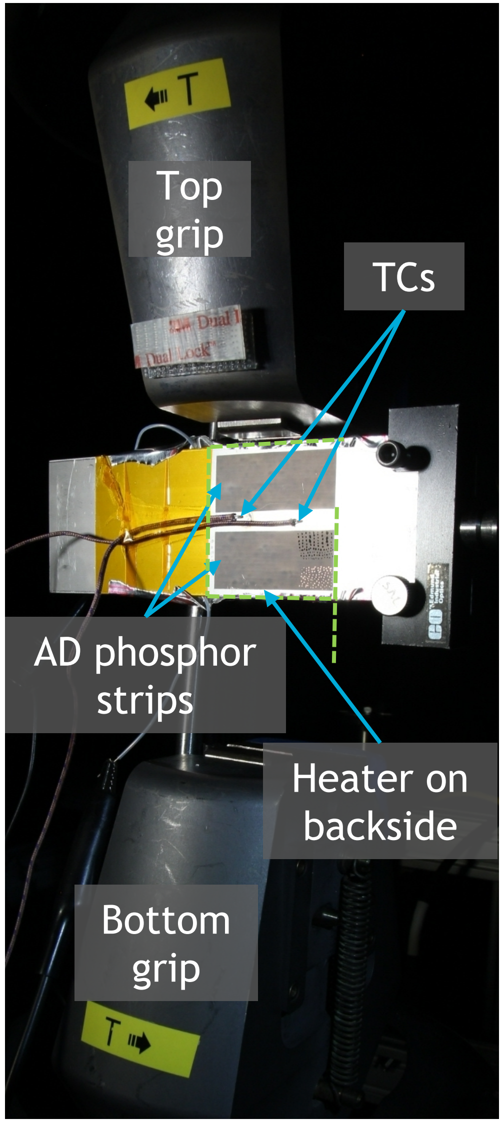

Representative pixel-wise calibration curves

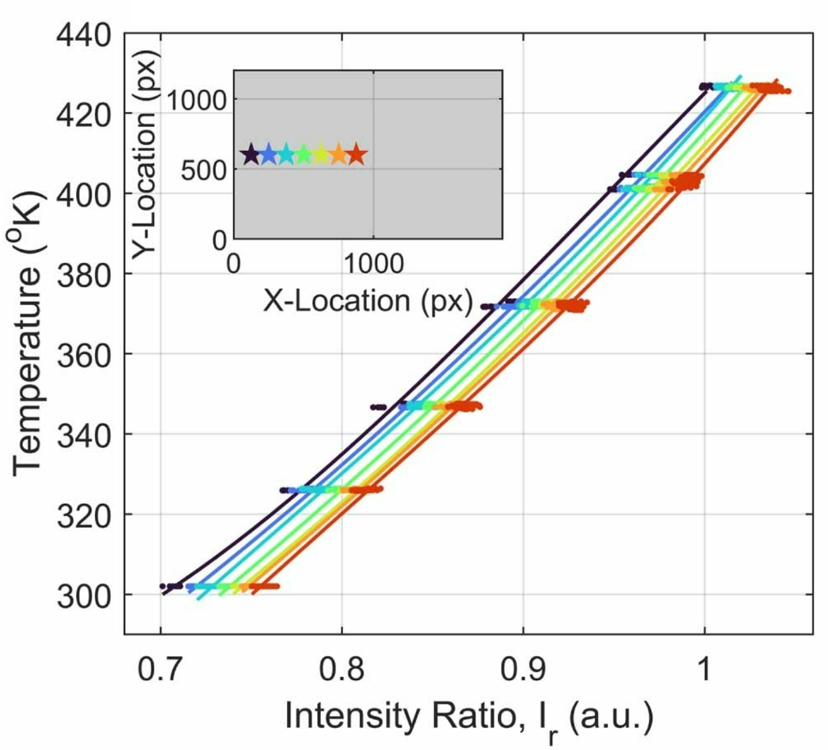

Standard deviation of inferred sample temperature

Area of interest (AOI): 400 < Y < 800 px

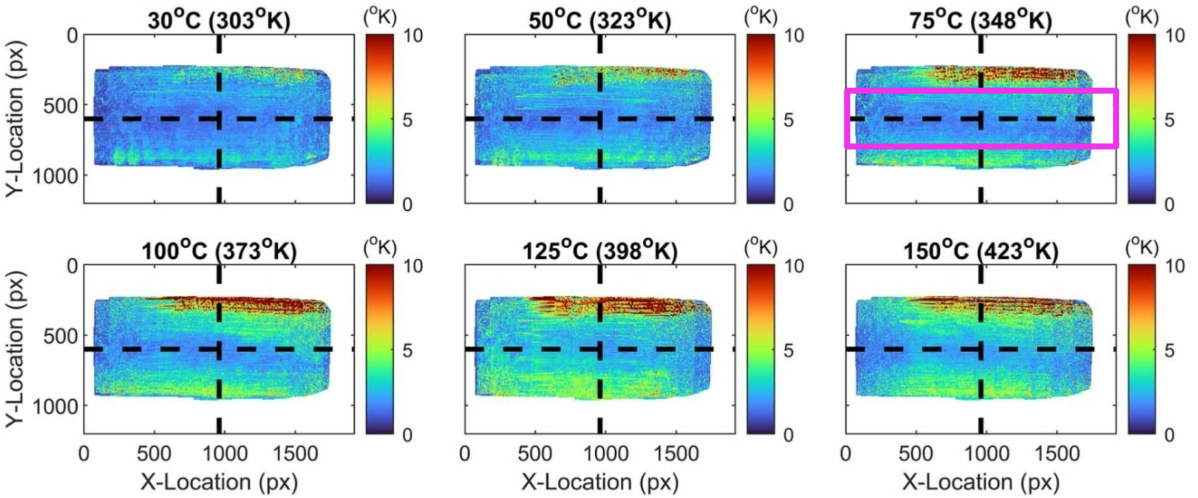

Physical Field of View: 55 x 90 mm

Temperature uncertainty of ± 3 K in AOI (the temperature sensitivity of the phosphor thermometry)

Jones, E. M. C., *Meas. Sci. Technol.*, 2022

E. Jones, C. Winters

Digital Image Correlation (DIC) Pattern for Strain Measurements

Patterned MFG phosphor coatings were applied by spraying through a Kapton mask with laser-cut holes

Spots as small as 0.25 mm diameter were successfully deposited

→ Demonstrates patterning can be achieved

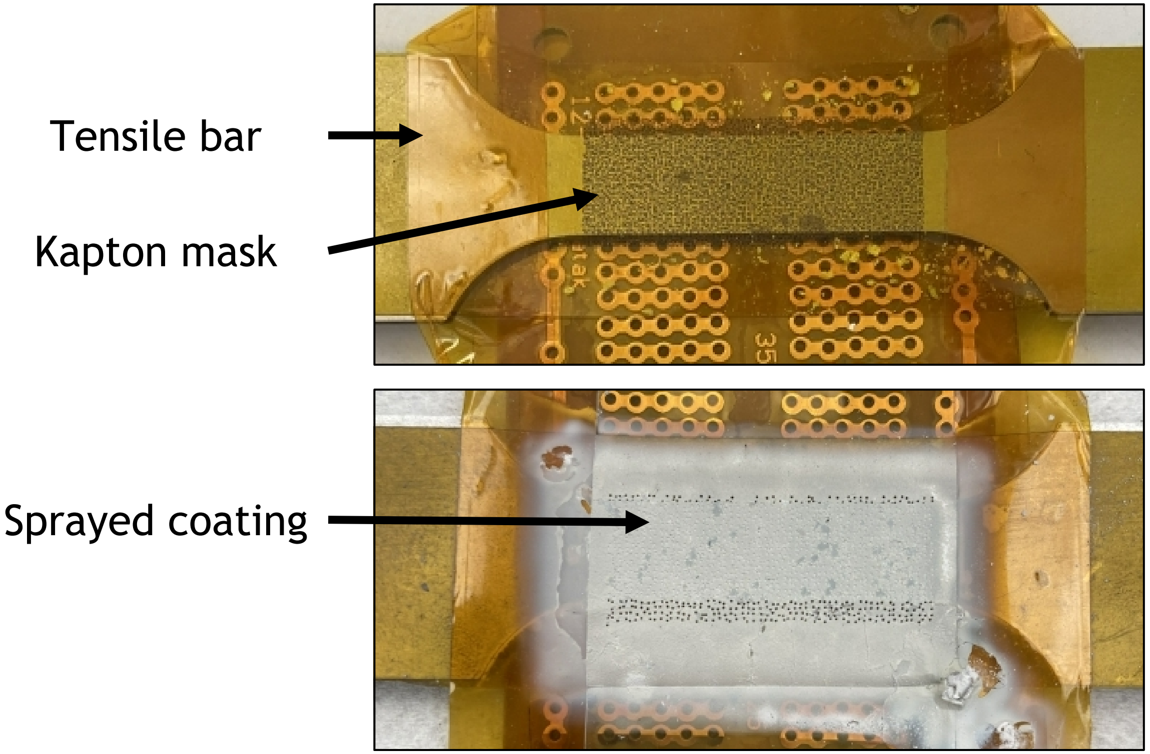

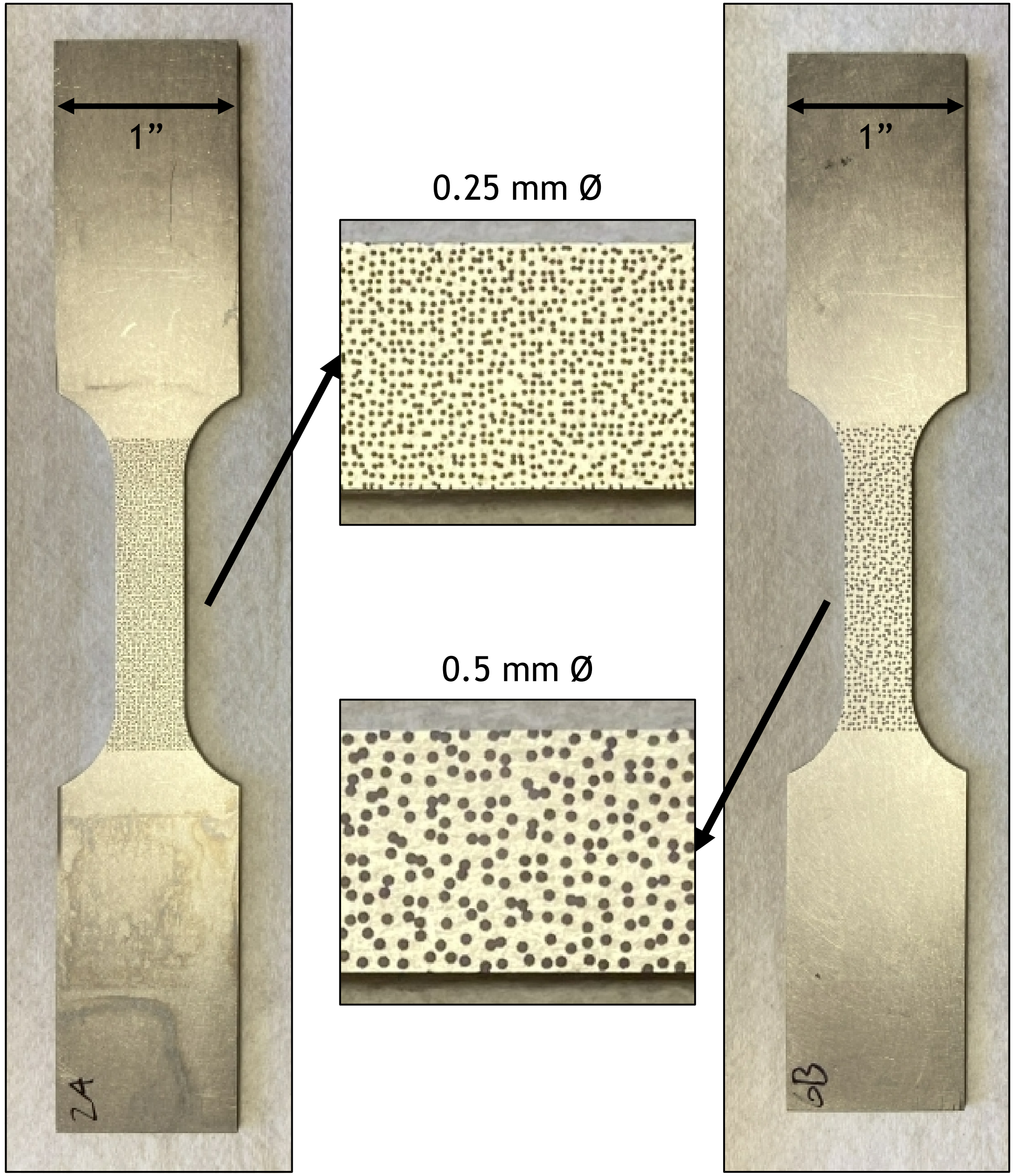

Simultaneous Temperature and Strain Measurements via Thermophosphor Digital Image Correlation (TP+DIC)

E. Jones, C. Winters

Before loading

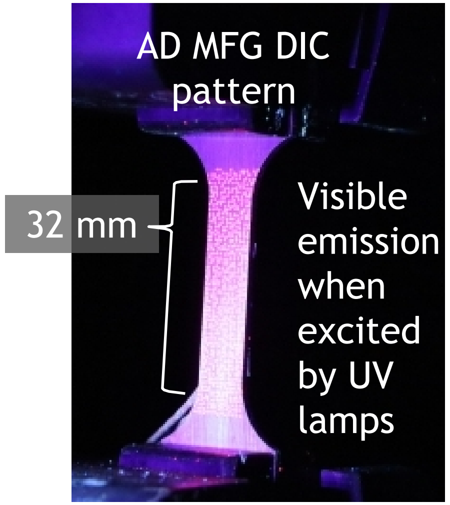

During loading

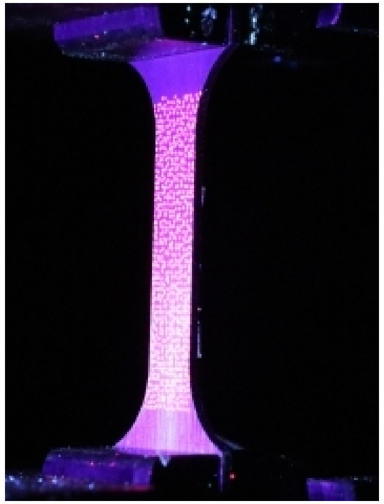

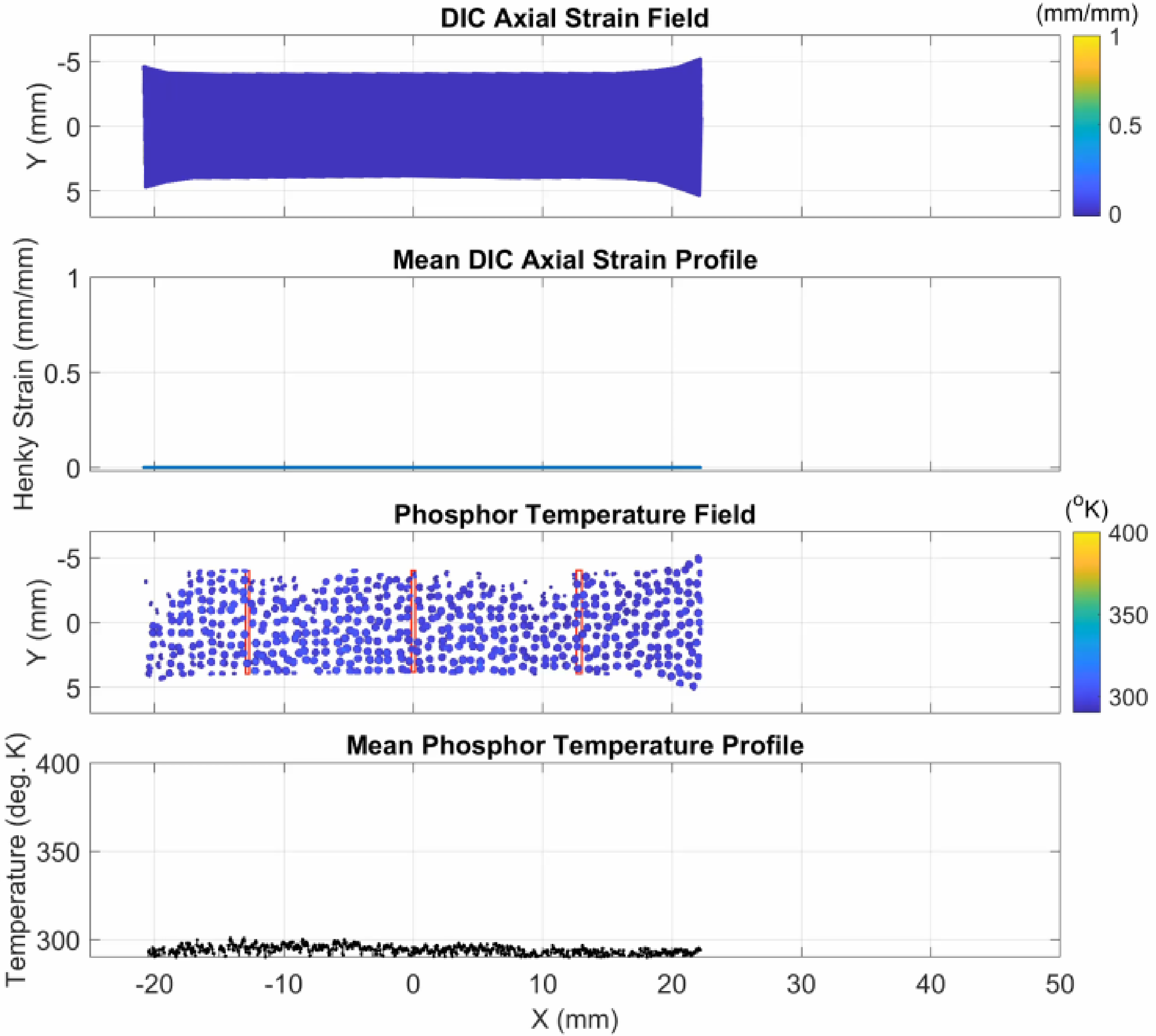

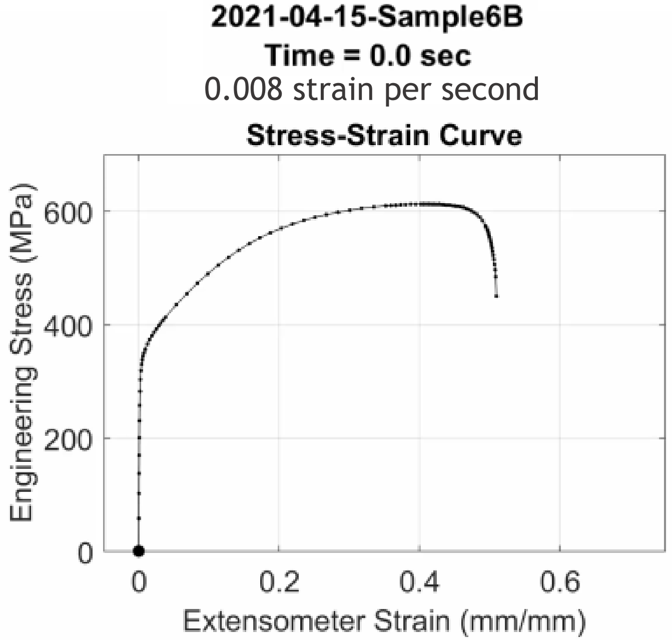

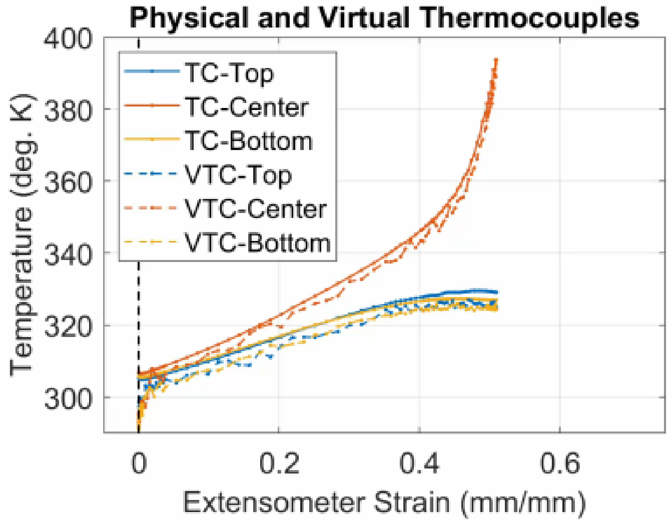

Jones, E. M. C., *Strain*, 2022

Processing Challenges for DIC Patterning

Mask holes filled with compacted powder

Powder deposited in the holes inhibits coating formation by subsequent passes

Resulting spots are easily wiped off the substrate

Solution: reduce powder feed rate and increase raster step size

Inconsistent powder feed can also result in compacted powder filling the mask holes

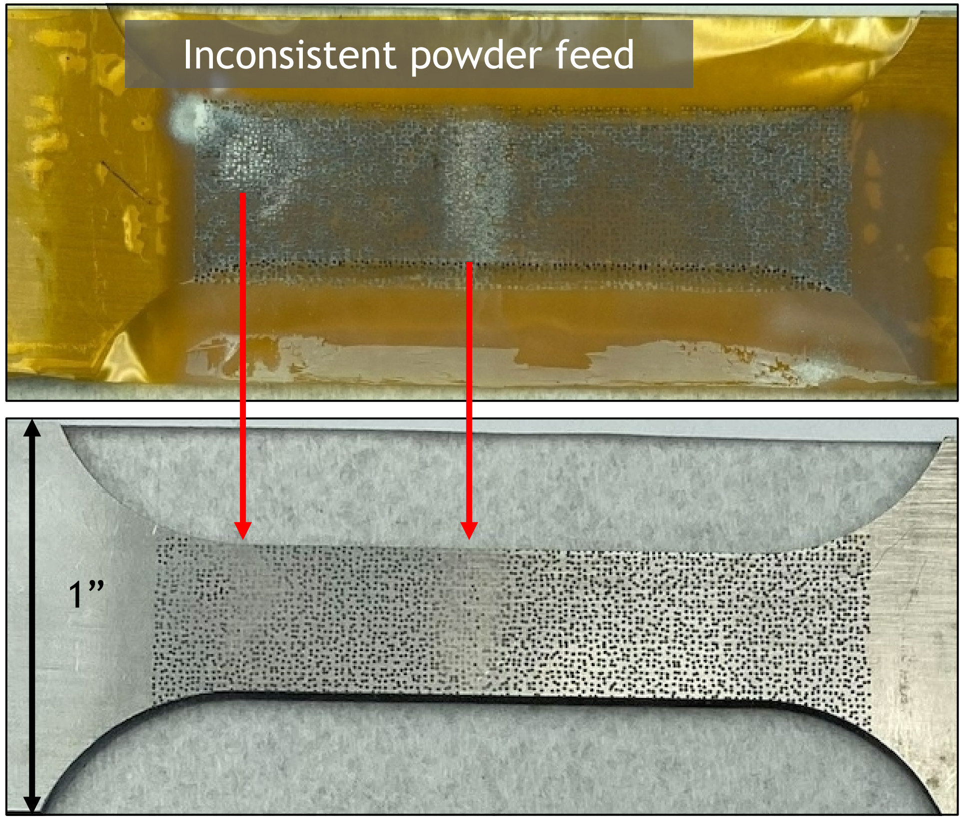

Uneven spot thickness

Even with successful deposition of the spots, the thickness of the spots varies across the sample

Future work: continue process development to further improve powder feed

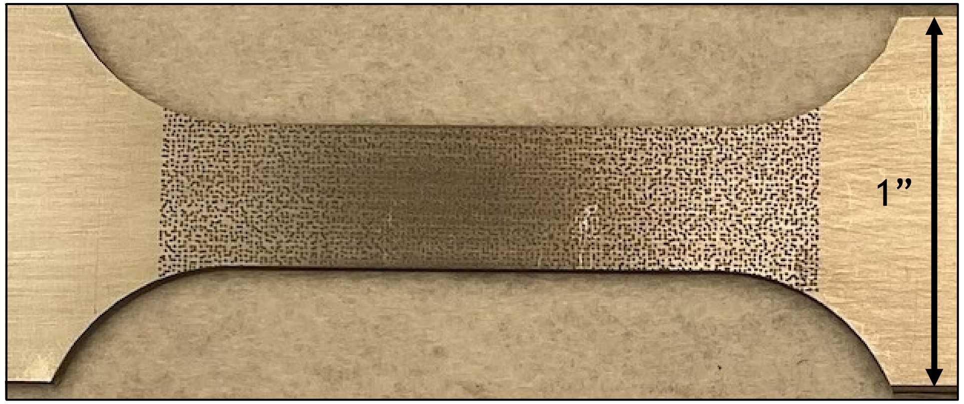

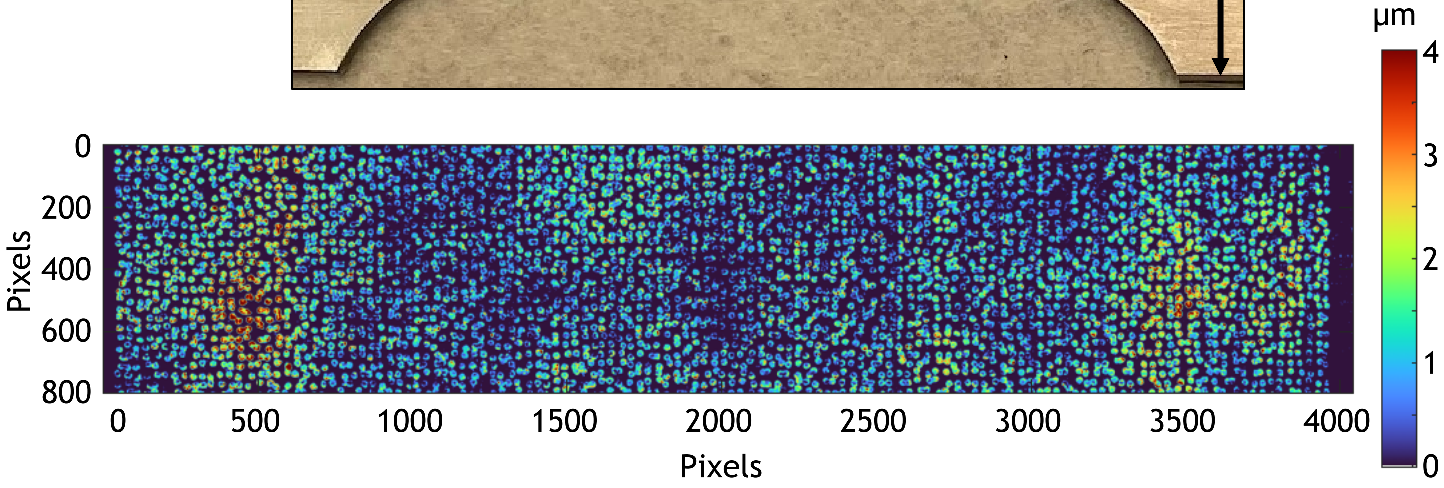

Outline

Background

1. Thermal Spray Research Laboratory
2. Aerosol Deposition
3. Thermographic phosphors

Previous Results

4. Deposition details
5. Temperature + strain measurements

Current Efforts

6. In-situ tensile test

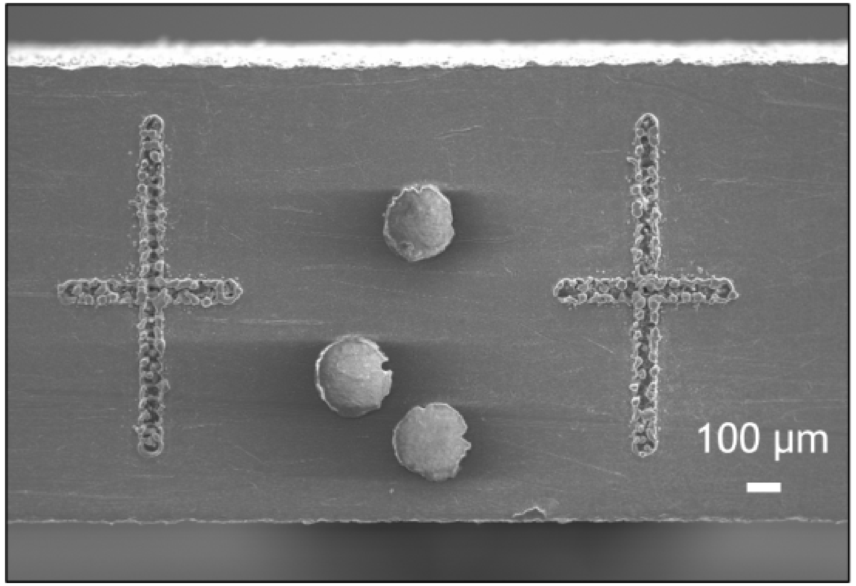

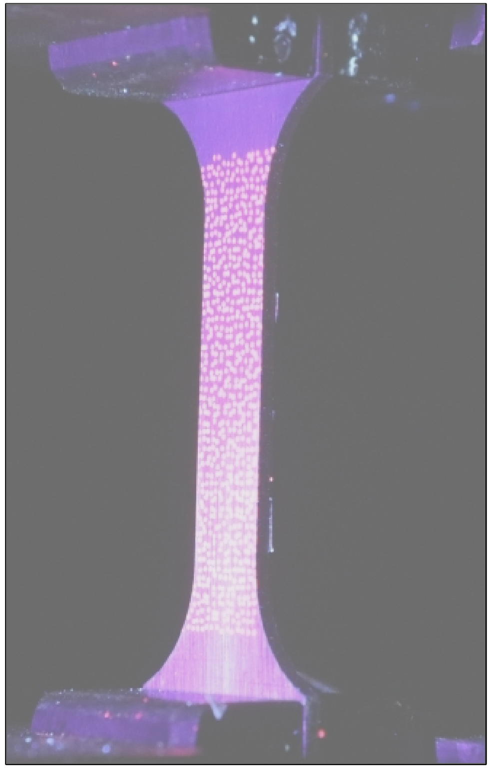

The spots crack but remain adhered during tensile testing

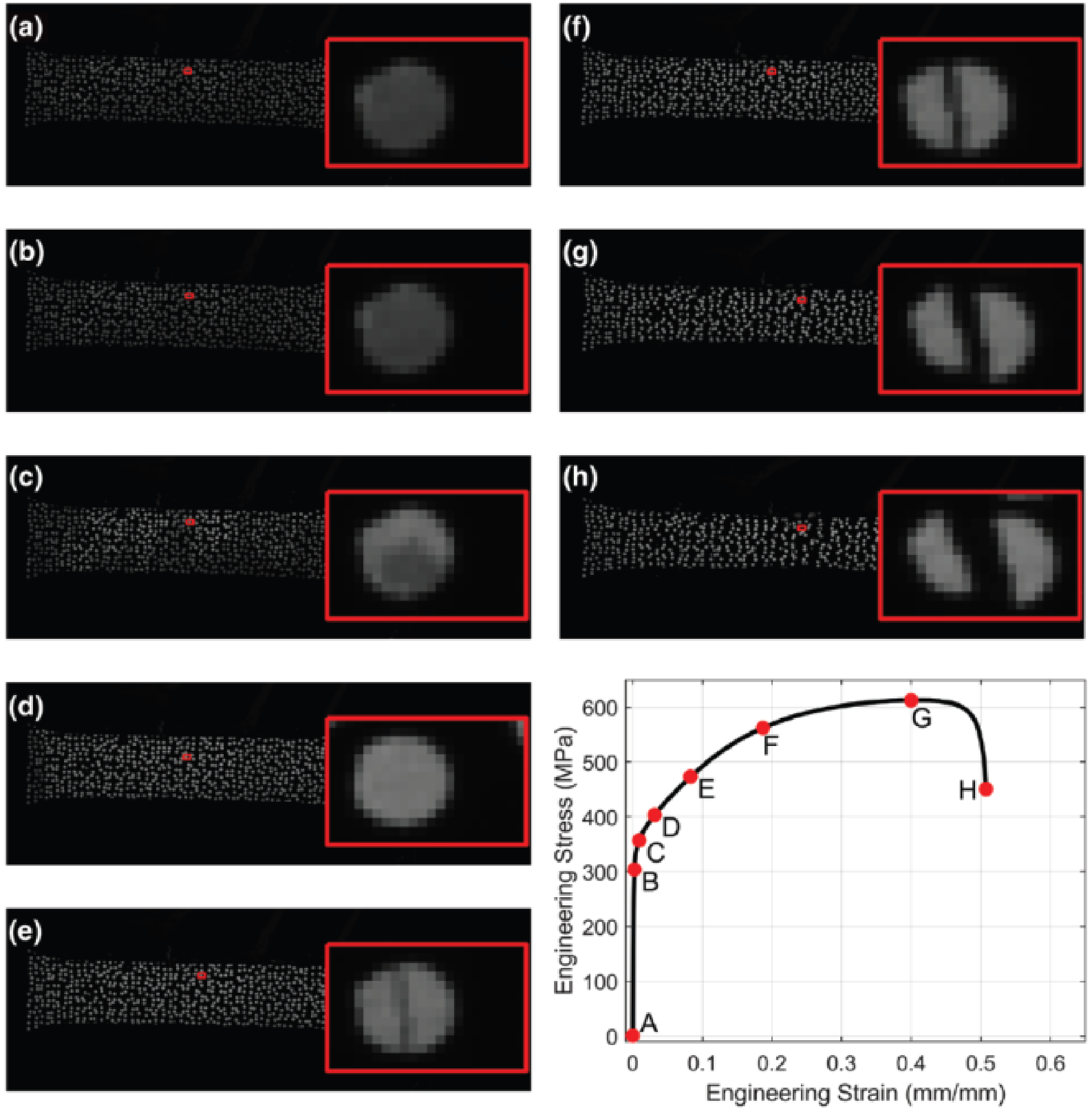

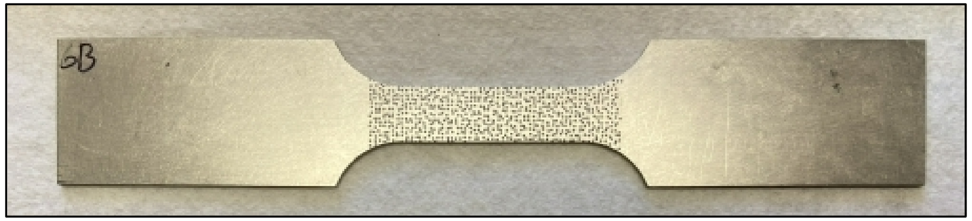

Tensile Test

MFG spots crack then move with the substrate during plastic deformation of the tensile bar

When the tensile bar fails, the spots delaminate

Use in-situ tensile tests in the scanning electron microscope to observe crack formation and propagation

Jones, E. M. C., *Strain* 2022

0.25 mm Diameter: Crack Formation and Propagation

Deposited 3 spots on a small steel tensile bar

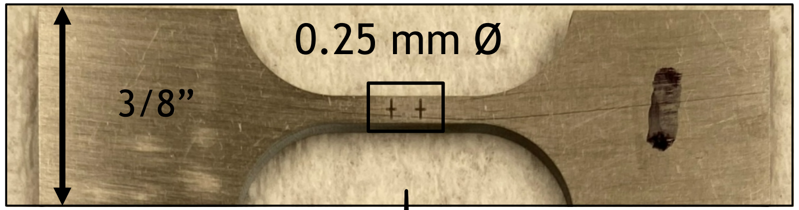

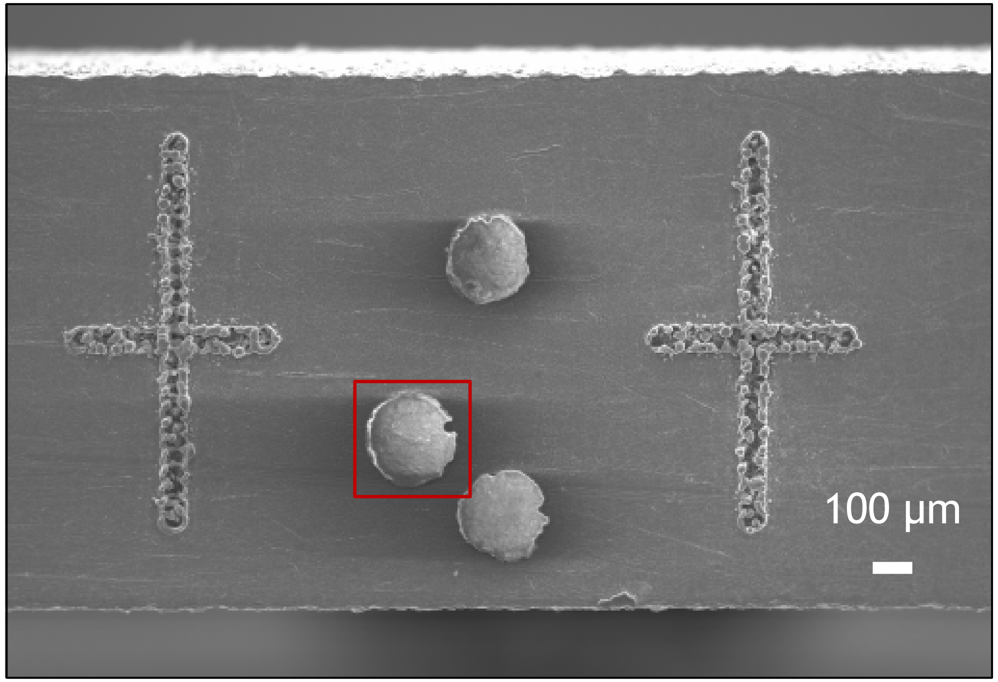

First appearance of cracks
Steel: 160 lb, 322 MPa, 0.0078 mm/mm

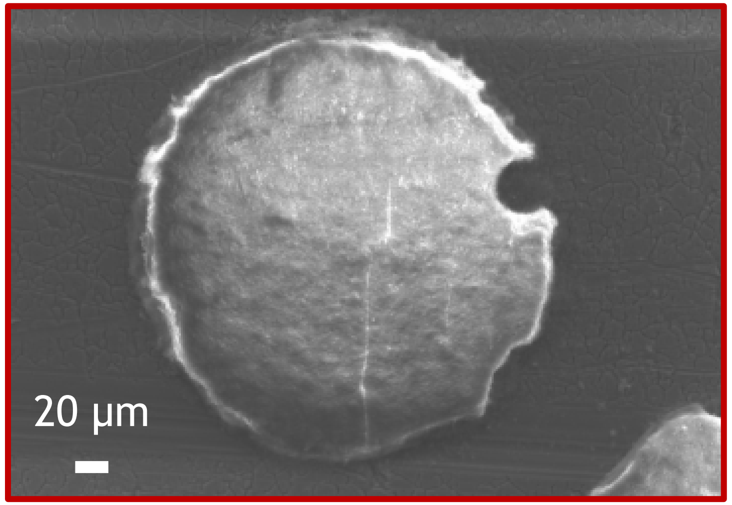

Cracks form perpendicular to the pull direction

Steel: 170 lb, 342 MPa, 0.0132 mm/mm

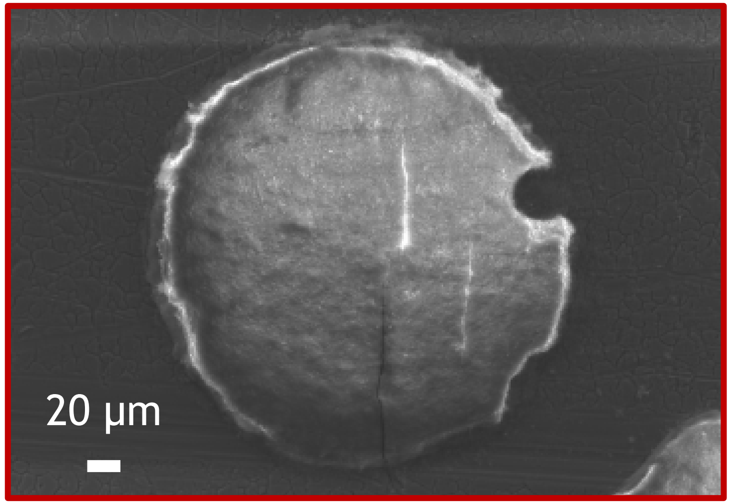

The original cracks grow as the tensile bar is pulled further

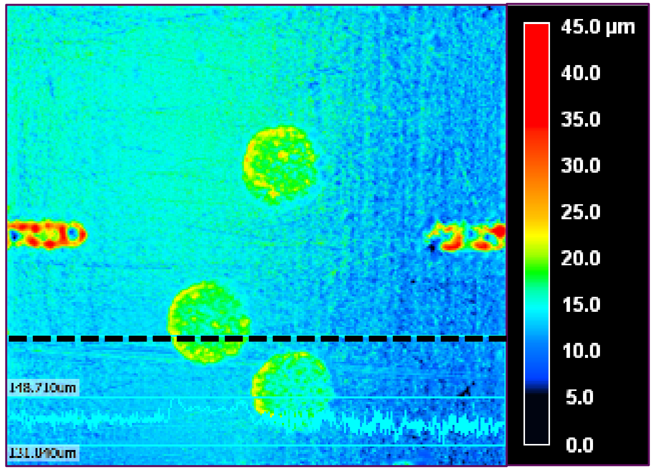

~4 microns thick

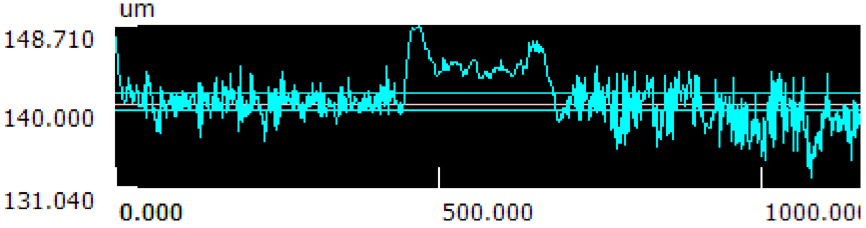

L. Jauregui, T. Ruggles

0.5 mm Diameter: Debonding

Deposited 1 spot on a small steel tensile bar

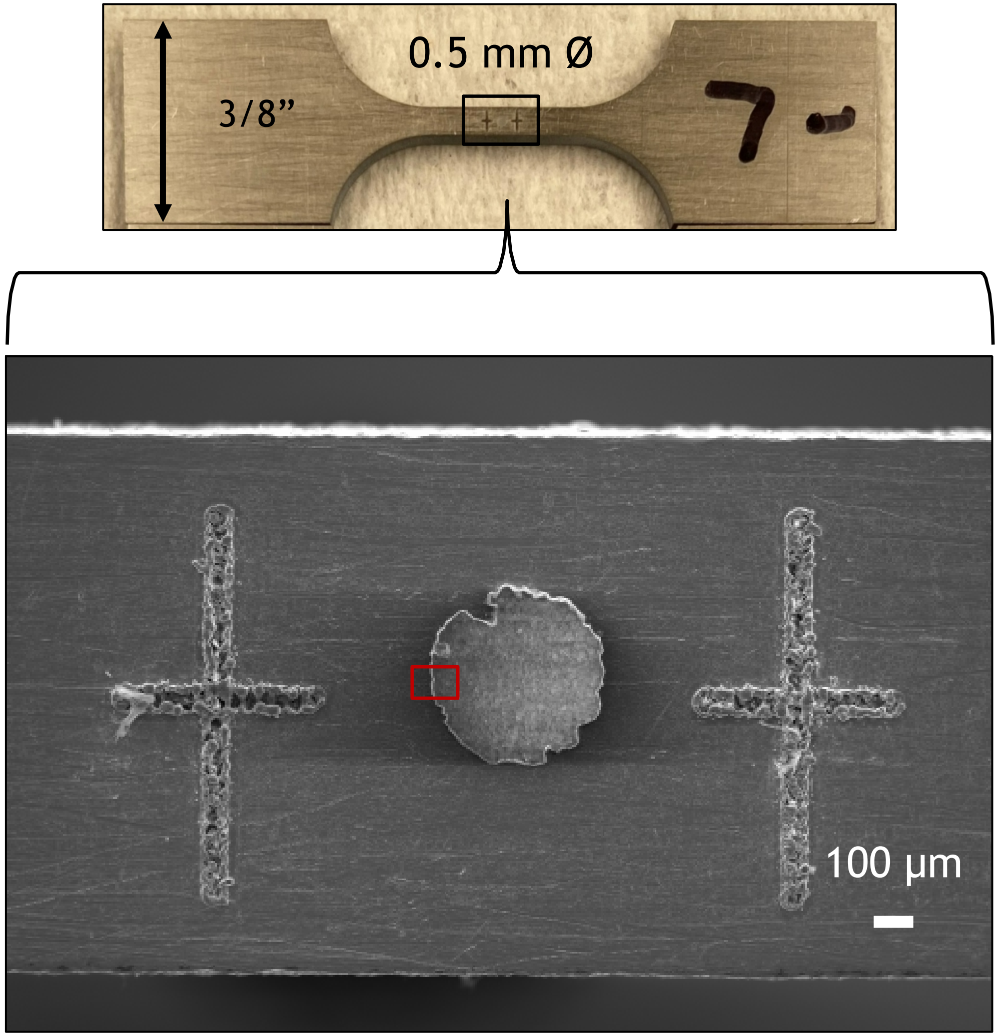

L. Jauregui, T. Ruggles

Debonding first observed at 170 lb, 342 MPa, 0.0163 m/m

Steel: 190 lb, 382 MPa, 0.0377 m/m

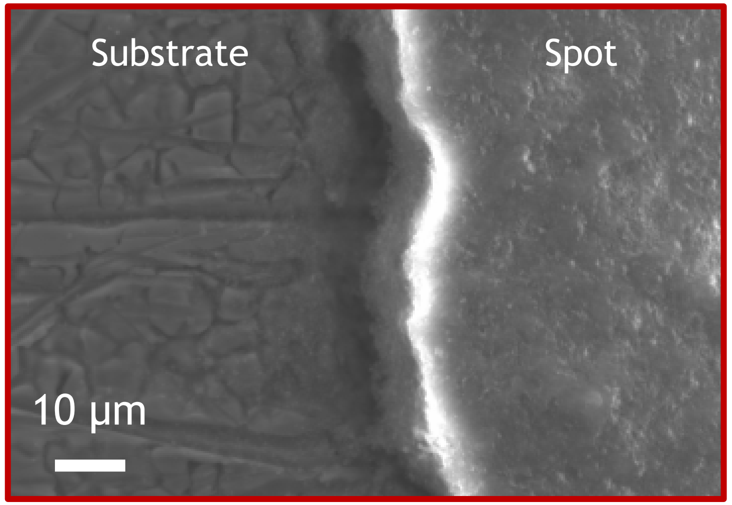

Steel: 250 lb, 503 MPa, 0.1327 m/m

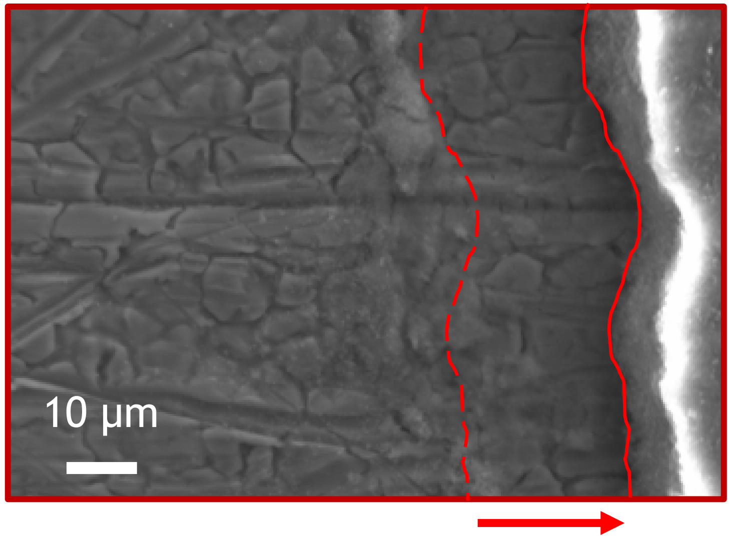

Edge of coating visibly shifts due to debonding

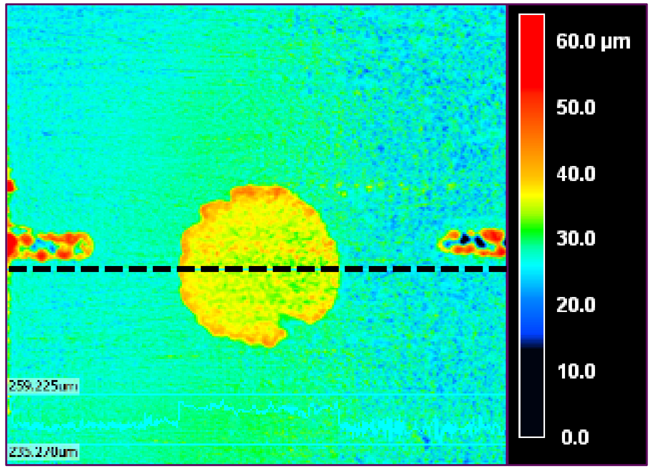

~7 microns thick

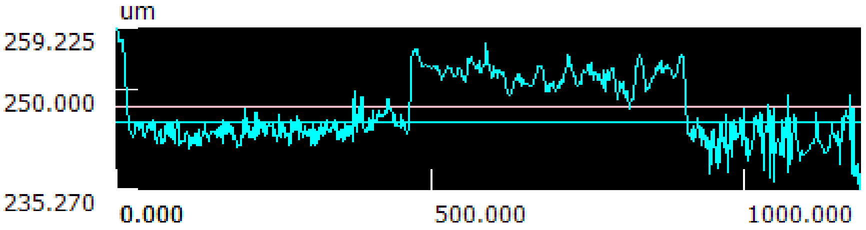

Future work: understand the effects of spot size vs spot thickness

Simultaneous temperature + strain sensing (TP+DIC) is a new and emerging application for AD coatings

AD coatings out-perform conventional phosphor coating methods

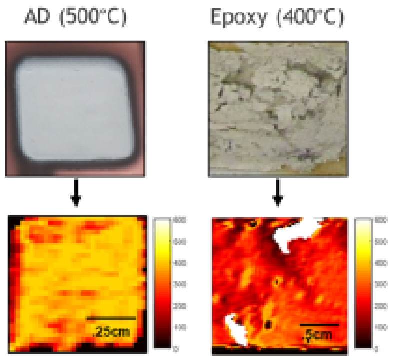

Highly sensitive and uniform temperature measurements

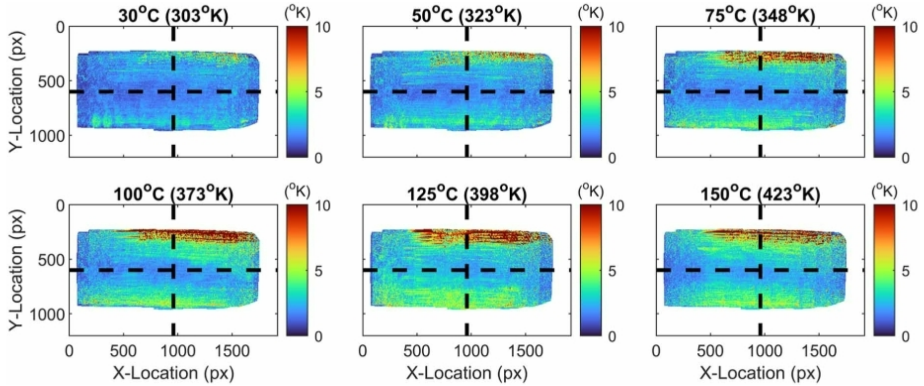

Simultaneous temperature and strain measurements

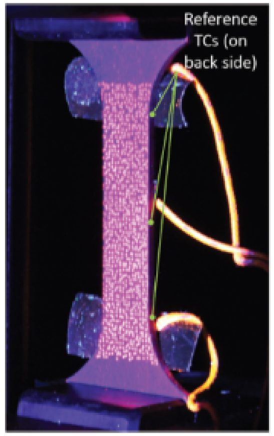

In-situ SEM experiments

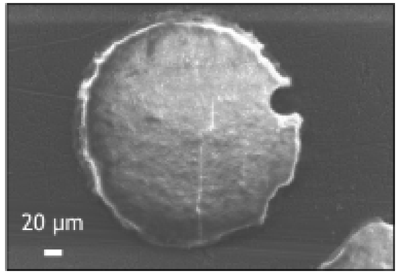

Contributors:
Jake Mahaffey, Caroline Winters, Elizabeth Jones, Amanda Jones, Kathryn Hoffmeister, Wendy Flores-Brito, Seth Davis, Abe Ramirez, Luis Jauregui, Tim Ruggles, Adrianna Gutierrez, Adrian Casias, Matt Swanson

Patent Application:
17/838,777, Thermographic phosphor digital image correlation

Publications:

- Jones, E. M. C., Jones, A. R., Winters, C., *Strain* 2022, e12415.
- Jones, E.M.C., Jones, A.R., Hoffmeister, K.N.G., Winters, C., *Meas. Sci. Technol.* 2022, 33, 085201
- Mahaffey, J., et al., *Proc. SPIE 11872, Advances in Optical Thin Films VII*, 2021, 118720M